This is an open access article published under an ACS AuthorChoice License, which permits copying and redistribution of the article or any adaptations for non-commercial purposes.

ACS central science

http://pubs.acs.org/journal/acscii

Research Article

Optimizing Strategy for Enhancing the Stability and $^{99}TcO_4^-$ Sequestration of Poly(ionic liquids)@MOFs Composites

Cheng-Peng Li, Hai-Ruo Li, Jin-Yun Ai, Jing Chen, and Miao Du*

Cite This: *ACS Cent. Sci.* 2020, 6, 2354−2361

Read Online

ACCESS | Metrics & More | Article Recommendations | Supporting Information

ABSTRACT: Metal−organic frameworks (MOFs) are a class of promising sorbents for effective sequestration of radioactive $^{99}TcO_4^-$ anions. However, their poor stability and slow sorption kinetics in the industrial condition pose a great challenge. Herein, we demonstrate an optimizing strategy via *in situ* polymerization of ionic liquids (ILs) encapsulated in the pores of MOFs, forming polyILs@MOFs composites with greatly enhanced TcO_4^- sequestration compared with the pristine MOFs. Notably, the cross-linked polymerization of ILs facilitates the formation of both the inside ionic filler as the active sites and outside coating as the protective layers of MOFs, which is significantly beneficial to obtain the optimized sorption materials of exceptional stability under extreme conditions (e.g., in 6 M HNO_3). The final optimized composite shows fast sorption kinetics (<30 s), good regeneration (>30 cycles), and superior uptake performance for TcO_4^- in highly acidic conditions and simulated recycle stream. This strategy opens up a new opportunity to construct the highly stable MOF-based composites and extend their applicability in different fields.

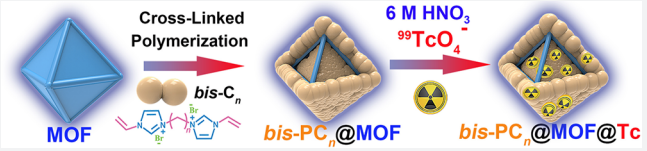

INTRODUCTION

Radioactive waste pollution, which is formed as the byproducts of the nuclear fuel industry and nuclear weapons, is one of the most severe threats to the international community.[1−4] The current proposed managing strategy of radioactive waste is very complicated by the inventory of long-living radionuclides, such as ^{99}Tc, because of its long half-life ($t_{1/2}$ = 2.1 × 10^5 years), high water solubility (11.3 M at 20 °C in the form of sodium salt), and serious perniciousness as low activity waste (LAW) under aerobic conditions.[5−8] Disposition of ^{99}Tc during the vitrification process of nuclear waste remains challenging due to the generation of volatile Tc_2O_7.[9] Therefore, ^{99}Tc removal from high-level waste steam prior to vitrification is greatly essential. The main form of ^{99}Tc in industry is pertechnetate ($^{99}TcO_4^-$), which can easily spread into the environment and enter into the food chain after accidental release. Notably, the large size and low charge density of TcO_4^- result in its low binding constant and the small complexing enthalpy in water, which makes it very difficult to be selectively recognized.[10−13] Removal of ^{99}Tc in groundwater is rather hard, because of the requirement to meet the low detection limit below the standard of drinking water (5.2 × 10^{-10} M or 900 pCi L^{-1}) defined by the U.S. Environmental Protection Agency.[14] Now, great success has been achieved on ^{99}Tc sequestration from alkaline solutions, especially the high-level nuclear waste stored in underground tanks at the Savannah River.[15−18] Nevertheless, it is still a great challenge to manage TcO_4^- species in highly concentrated HNO_3 medium, prior to the plutonium uranium redox extraction (PUREX) process.[19,20]

For the established technologies for TcO_4^- remediation, the utilization of solid sorbents holds great promise, considering their simple, safe, and low-cost processes and superior performances for removal of anions at a low concentration level and point-of-use applications.[21−27] Although the pioneering endeavor of this topic was explored long ago, it is definitely a long-term battle for ^{99}Tc decontamination. As a matter of fact, the traditional commercialized polymeric anion-change resins (e.g., superLig-639 or Purolite-A-520E) have slow anion-exchange kinetics and poor radiation resistance.[28,29] The inorganic cationic materials, such as the layered double hydroxides (LDHs) or layered rare-earth hydroxides (LRHs), possess a limited sorption capability and poor selectivity.[30,31] As an emerging candidate to sequester TcO_4^- from nuclear waste, metal−organic frameworks (MOFs) are endowed with the unique advantages of tailored porous structures and facile functionalization, relying on their modular building blocks.[32−35] Some cationic MOFs exhibit good sorption capability and selectivity to pertechnetate, but slow kinetics, low stability, and poor recyclability under highly acidic conditions.[36−38]

In fact, most MOF materials are constructed by carboxylate- or azolate-involved ligands and thus have the neutral porous frameworks. Considering the available database of numerous MOFs, it can be envisioned that the incorporation of cationic polymers into neutral MOFs will afford diverse composites,

Received: October 6, 2020
Published: November 30, 2020

ACS Publications

© 2020 American Chemical Society

which can serve as the anion receptors with high density of easily accessible anion-exchange sites. This strategy may also endow the porous composites with fast sorption kinetics and high stability.[39,40] Nevertheless, a simple incorporation of cationic polymers into MOFs will suffer from the size incompatibility, owing to the limited open windows of MOFs. On the other hand, several cationic monomers have been used to bind to the organic ligands in MOFs, either prior to or after the synthesis of MOFs, to obtain polymers@MOFs composites.[41−44] However, either the complex synthetic procedure or the need of a special active group largely limits their universal applications. As a result, a more feasible approach has been developed to fabricate polymers@MOFs composites, by encapsulating the small monomers into MOFs in advance and then implementing polymerization *in situ*. In this way, the intrinsic properties of both polymers and MOFs could be reserved in the resultant composites.[45−48]

To demonstrate the above proof-of-concept for the design of anion sorbents, in this work, imidazolium-based ionic liquids (ILs) were used as the monomers given their cationic nature, tunable sizes, and easy-to-obtain properties.[49] Besides these, ILs could be easily impregnated to the pores of MOFs, even under the vacuum condition,[50] due to their liquid nature and extremely low vapor pressure. Moreover, the interactions between ILs and pore walls of MOFs allow the immobilization of ILs into MOFs.[51] Up to now, some ILs@MOFs or polyILs@MOFs composites have been developed for catalysis, gas adsorption/separation, and ion conduction.[47,52,53] In the reported examples, ILs or polyILs are normally considered to be entrapped within the MOFs due to size confinement.[54,55] Thus, the leaching of ILs or polyILs under industrial conditions is a significant problem to the practicability of composites. Also, the performances of such composites will be greatly affected by their stability toward water and acidic or alkaline solutions.

With the above points in mind, cross-linked polyILs@MOFs composites can be constructed and applied in pertechnetate sequestration, considering the following features: (i) The high density of anion-exchange sites of polyILs and hierarchical porosity of composites could facilitate a rapid anion transportation. (ii) The *in situ* generated cross-linked polymers may improve the stability of composites. (iii) The highly cross-linked polymers and hydrophobic pores of MOFs afford a high affinity to the less hydrated anion (e.g., TcO_4^-) to enhance the selectivity. To establish the structure−property relationship and optimize the sorption performances, a variety of ILs (linear or cross-linked monomers) and MOFs (MIL-101, UiO-66, and ZIF-8) were employed for de novo synthesis. Notably, the polyILs@MOFs composites integrate the advantages of each individual component, with highly enhanced sorption kinetics, uptake capacity, stability, and recyclability under extreme conditions, toward TcO_4^- or ReO_4^- (a nonradioactive surrogate for TcO_4^-) remediation. Further, an optimizing strategy to enhance the stability and reusability for MOF-based composites was proposed, which can be generally applied in different fields.

RESULTS AND DISCUSSION

Synthesis and Characterization. The targeted polyILs@MOFs sorbents were obtained by impregnation of ILs into MOFs and then *in situ* polymerization (see Figure 1). By this approach, the polyILs@MOFs composites with different structural features and adsorption performances could be

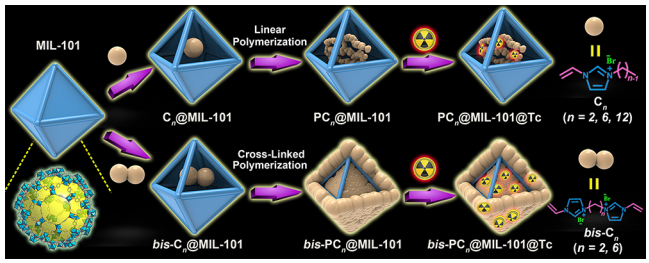

Figure 1. Designing strategy of polyILs@MOFs composites for radionuclide sequestration, by *in situ* polymerization of the encapsulated imidazolium-based ILs in the pores of MOFs (MIL-101 was chosen as the representative MOF here).

easily achieved, through changing the IL monomers and/or MOF precursors. In this work, we chose two series of imidazolium-based monomers, including the linear species bearing one vinyl group (C_n, n = 2, 6, and 12) and the cross-linked species bearing two vinyl terminals (*bis*-C_n, n = 2 and 6) with the following considerations (Figure 1): (i) Such polyILs in hierarchical pores of polyILs@MOFs have the rich positive charges, therefore enhancing the sorption kinetics of anions. (ii) The cross-linked polymers may coat on the surface of MOFs, thus protecting MOFs in extreme conditions. (iii) The ILs modified with different substituents in polyILs@MOFs composites may affect their sorption ability, thus providing the opportunities to optimize these sorbents. As a result, two series of PC_n@ MOFs and *bis*-PC_n@MOFs composites (here, MOFs = MIL-101, UiO-66, or ZIF-8) can be achieved. Prior to the anion-exchange, the toxic Br^- anion in composites was replaced with the Cl^- ion, via treating with the saturated NaCl solution. Herein, PC_2(Cl)@MIL-101 and *bis*-PC_2(Cl)@MIL-101 were selected as the representatives for a thorough illustration, owing to their superior sorption capabilities. The enhanced sorption capacities were also observed in polyILs@UiO-66 and polyILs@ZIF-8, compared with the corresponding pristine MOFs, which thus were enumerated to confirm the universality of the proposed strategy.

FT-IR spectra were taken to illustrate the polymerization of monomers in MIL-101. All characteristic peaks of *bis*-C_2 and MIL-101 can be observed in the FT-IR spectrum of *bis*-C_2@MIL-101, where the peaks at 925 and 978 cm^{-1} reveal the bending vibrations of $=CH_2$ and =C—H groups, respectively (Figure 2a). Upon polymerization, the two peaks are clearly weakened in *bis*-PC_2(Cl)@MIL-101 and *bis*-PC_2. With regard to *bis*-PC_2@MIL-101@Re, the peak at 910 cm^{-1} corresponds to the adsorbed ReO_4^- anions. Similar results were also observed in the FT-IR spectra of PC_n@MIL-101 (n = 2, 6, and 12) and *bis*-PC_6@MIL-101 composites (Figure S1). Additionally, PXRD patterns illustrate the framework integrity of composites (Figure 2b and Figure S2). Their porosity was evaluated by N_2 adsorption isotherms at 77 K (Figure 2c). The Brunauer−Emmett−Teller (BET) surface areas are significantly reduced for *bis*-PC_2(Br)@MIL-101 (1055 $m^2\ g^{-1}$) and *bis*-PC_2(Cl)@MIL-101 (1891 $m^2\ g^{-1}$), compared with that of MIL-101 (2926 $m^2\ g^{-1}$), due to the introduction of polyILs. The larger Br^- anions result in a smaller BET surface area of *bis*-PC_2(Br)@MIL-101, compared with *bis*-PC_2(Cl)@MIL-101. Moreover, compared with MIL-101, the pore volumes of *bis*-PC_2(Br)@MIL-101 and *bis*-PC_2(Cl)@MIL-101 show a shrinkage due to the occupation of voids in MIL-101 by polyILs (Figure S3). Such hierarchical pores in polyILs@MIL-101 facilitate the anion transportation and/or sorption. The

https://dx.doi.org/10.1021/acscentsci.0c01342
ACS Cent. Sci. 2020, 6, 2354−2361

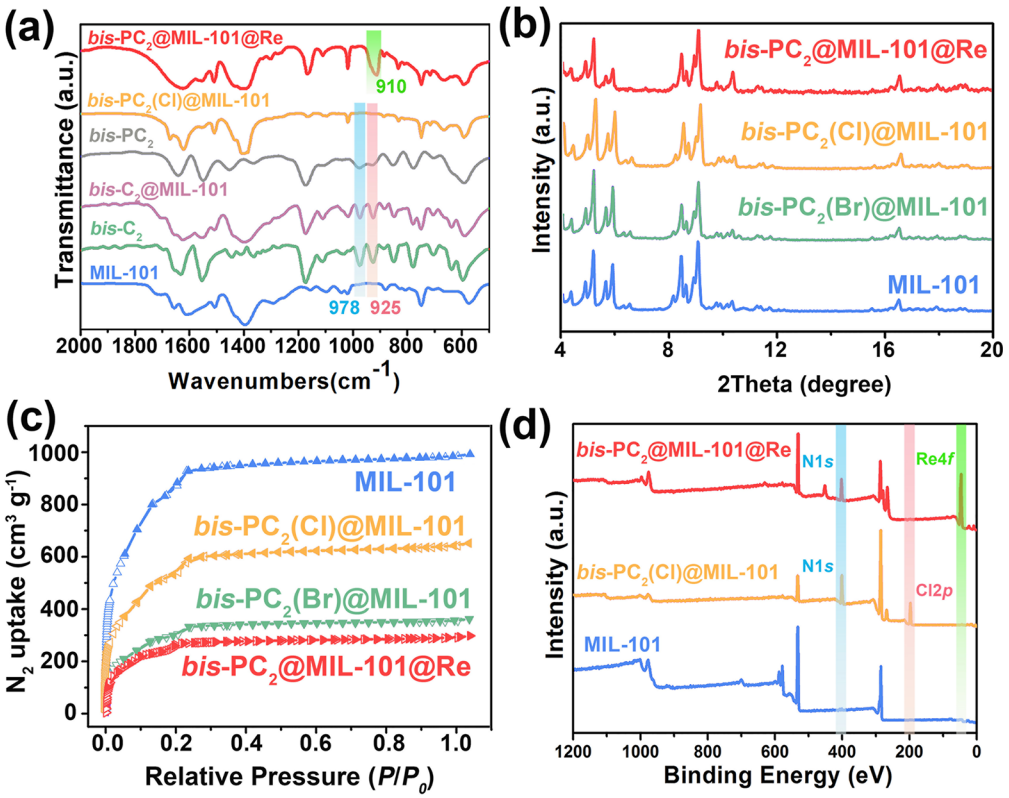

Figure 2. (a) FT-IR spectra of MIL-101, *bis*-C_2, *bis*-C_2@MIL-101, *bis*-PC_2, *bis*-PC_2(Cl)@ MIL-101, and *bis*-PC_2@MIL-101@Re. (b) PXRD patterns and (c) N_2 sorption isotherms of MIL-101, *bis*-PC_2(Cl)@MIL-101, *bis*-PC_2(Br)@MIL-101, and *bis*-PC_2@MIL-101@Re. (d) XPS survey spectra of MIL-101, *bis*-PC_2(Cl)@MIL-101, and *bis*-PC_2@MIL-101@Re.

BET surface area of *bis*-PC_2@MIL-101@Re is further decreased to 875 m^2 g^{-1}, and a continuous shrinking of pore volume is found after anion uptake. This can be attributed to the void consumption and mass increment after ReO_4^- sorption. XPS was employed to investigate the chemical compositions of MIL-101, *bis*-PC_2(Cl)@MIL-101, and *bis*-PC_2(Cl)@MIL-101@Re (Figure 2d). Compared to MIL-101, the XPS survey for *bis*-PC_2(Cl)@MIL-101 shows the additional peaks of N 1s (401.3 eV) and Cl 2p (197.1 eV), revealing the existence of imidazolium and Cl^-. Moreover, the appearance of Re 4f peaks and disappearance of Cl 2p peak in XPS of *bis*-PC_2(Cl)@MIL-101@Re indicate the complete anion-exchange of Cl^- by ReO_4^-. For free ReO_4^-, the XPS signals of Re $4f_{5/2}$ and Re $4f_{7/2}$ are observed at the binding energies of 48.3 and 45.9 eV,[56] which shift to 48.4 and 46.0 eV, respectively, for *bis*-PC_2@MIL-101@Re (Figure S4). This result clearly reveals a decrease of electron density of ReO_4^- in *bis*-PC_2@MIL-101@Re, caused by the interactions between ReO_4^- and *bis*-PC_2@MIL-101 in the composite.

To gain a better understanding of ILs' entrapment within MIL-101, STEM-EDS images of MIL-101 and polyILs@MIL-101 were further performed (Figures S5−S7). The *in situ* linear polymerization of C_2−ILs occurs in the inner void of MIL-101, and the formed PC_2 polymer is not observed on the crystal surface (Figure S5). By introducing a mixture of C_2 and *bis*-C_2 IL monomers, most of the formed polyILs are located within the pores of MIL-101, whereas a few polyILs cover on the surface of MOF particles (Figure S6). By contrast, the use of cross-linked *bis*-C_2 monomers affords the *bis*-PC_2@MIL-101 composite, where the surface of MIL-101 crystals is coated by a mass of polyILs (Figure S7). Notably, the toxic Br^- in polyILs@MIL-101 could be fully replaced by Cl^-, which motivates us to explore its application in radionuclide polluted water treatment. The TGA curve (Figure S8) also confirms the presence of ILs in the pores of *bis*-PC_2(Cl)@MIL-101, showing additional weight loss of 13.2% at ca. 300 °C that is not observed for MIL-101.

Sorption Kinetics. The sorption experiments of TcO_4^- ions were initially performed by mixing 5 mg of *bis*-PC_2(Cl)@MIL-101 with 5 mL of aqueous solution containing 26 ppm TcO_4^-. The concentration of TcO_4^- in solution was traced by the UV−vis characteristic peak at 290 nm and liquid scintillation counting (LSC) measurements. As depicted in Figure 3a, *bis*-PC_2(Cl)@MIL-101 shows an extremely high removal rate for the TcO_4^- anion and the UV−vis characteristic peak at 290 nm fully disappears within 30 s, which is the fastest limitation for the manual experimental operation. This result is comparable to that of SCU-CPN-1,[57] an anion-exchange polymer with the fastest TcO_4^- sorption kinetics and shortest equilibrium time thus far. For *bis*-PC_2(Cl)@MIL-101, the cationic polyILs coated on the outside of the MOF particles and easily attract TcO_4^- in solution via electrostatic interactions. Then, the attracted TcO_4^- anions enter into the channels of the composite, which are trapped by the inner network. Thus, the polymeric components and the hierarchical pores in *bis*-PC_2(Cl)@MIL-101 should account for the rapid anion transportation. For the similarity in both magnitude and trend in solubility of TcO_4^- and ReO_4^- anions, *bis*-PC_2(Cl)@MIL-101 shows similar sorption kinetics for two such anions (Figure S9). The experiment was initially performed by mixing 2 mg of *bis*-PC_2(Cl)@MIL-101 with a 5 mL water solution of 50 ppm ReO_4^-. The ReO_4^- sorption kinetics data can be fitted

https://dx.doi.org/10.1021/acscentsci.0c01342
ACS Cent. Sci. 2020, 6, 2354−2361

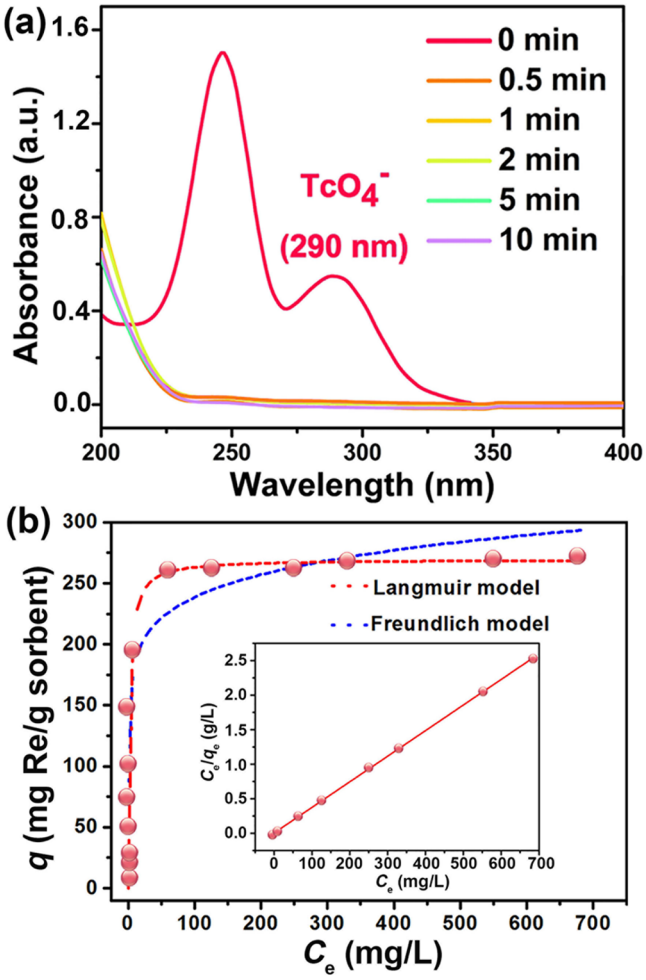

Figure 3. (a) UV−vis spectra of the TcO_4^- solution during anion-exchange by *bis*-PC_2(Cl)@MIL-101. (b) Sorption isotherm of *bis*-PC_2(Cl)@MIL-101 for ReO_4^-. Inset: linear regression by fitting the equilibrium data with the Langmuir sorption model.

by using the pseudo-second-order model, with a high correlation coefficient of >0.9999 (Figure S10 and Table S1). The rate constant k_2 of 22.03 g mg^{-1} min^{-1} shows an ultrafast sorption rate. The distribution coefficient K_d of *bis*-PC_2(Cl)@MIL-101 is 3.3×10^6 mL g^{-1}, which is comparable to PQA-*p*N$(Me)_2$Py-Cl (1.0×10^7 mL g^{-1}) that represents the highest performance now.[58] To evaluate its real application for the instant radionuclide sequestration, a chromatographic column was fabricated with *bis*-PC_2(Cl)@MIL-101 as the stationary phase. Notably, the water solution of ReO_4^- (188 ppm) could be successfully purified (95.4% removal), via simply passing it through the column under ambient pressure (Figure S11). In contrast, most known sorbents require lengthy contacting time and vigorous stirring to this aim, which are clearly unfavorable for the fast treatment of slightly contaminated water.

Due to the limited availability and high radioactivity of $^{99}TcO_4^-$, ReO_4^- was used in the experiment of the sorption isotherm. It was initially taken by mixing *bis*-PC_2(Cl)@MIL-101 (5 mg) with a water solution of TcO_4^- (5 mL) at a certain concentration (0−1000 ppm). The sorption of ReO_4^- by *bis*-PC_2(Cl)@MIL-101 follows the Langmuir isotherm model (Figure 3b), with a high correlation coefficient of >0.99 (Table S2). The sorption capacity is 270 mg of Re per gram of sorbent, which corresponds to 362 mg of ReO_4^- per gram of sorbent. This value amounts to ca. 5 times that found in MIL-101 (55 mg of Re per gram of sorbent), indicating the great advantages of the composite optimization strategy. Notably, *bis*-PC_2 has a good water solubility, which thus cannot be used for ReO_4^- sorption in water.

Sorption Mechanism. To reveal the sorption mechanism, a comprehensive comparative study on ReO_4^- sorption of MIL-101, PC_2(Cl)@MIL-101, PC_2(Cl)/*bis*-PC_2(Cl)@MIL-101, and *bis*-PC_2(Cl)@MIL-101 (Figure 4a) was taken under similar conditions (5 mg of sorbents; 5 mL aqueous solution of 200 ppm ReO_4^-). The removal percentages for the ReO_4^- ion follow the order *bis*-PC_2(Cl)@MIL-101 (99.86%) > PC_2(Cl)/*bis*-PC_2(Cl)@MIL-101 (79.03%) > PC_2(Cl)@MIL-101 (64.98%) > MIL-101 (53.49%), as shown in Table S3. Accordingly, the values of distribution coefficient (K_d) and rate constant (k_2) of *bis*-PC_2(Cl)@MIL-101 are 642 and 87 times more than those of MIL-101. The remarkable increments in ReO_4^- uptake capacity and rate can be well ascribed to the presence of cross-linked polymers in *bis*-PC_2(Cl)@MIL-101. To confirm this assumption, a full study on serial polyILs@MIL-101 composites was taken. As a result, both the ReO_4^- removal percentages and K_d values follow the order (Table S3) *bis*-PC_2(Cl)@MIL-101 > PC_2(Cl)/*bis*-PC_2(Cl)@MIL-101 > *bis*-PC_6(Cl)@MIL-101 > PC_2(Cl)@MIL-101 > PC_6(Cl)@MIL-101 > PC_{12}(Cl)@MIL-101. Based on these results, the composites of *bis*-PC_n@MIL-101 produced from ILs with two vinyl groups show better sorption performances due to the cross-linked polymerization. In comparison, those single-chain polymers in PC_n@MIL-101 may partially pass through the pores and transfer to the water solution during anion-exchange. On the other hand, with the increment of the spacers in ILs of C_n (n = 2, 6, and 12) and *bis*-C_n (n = 2 and 6), the resultant polyILs have the lower charge density, thus reducing the sorption efficiency of composites. To demonstrate the universality of this optimizing strategy, two other well-known MOFs (UiO-66 and ZIF-8) and their composites *bis*-PC_2(Cl)@UiO-66 and *bis*-PC_2(Cl)@ZIF-8 were explored by sorption tests (Figure 4a and Table S3). The ReO_4^- removal percentages by *bis*-PC_2(Cl)@UiO-66 and *bis*-PC_2(Cl)@ZIF-8 are 7 and 181 times, respectively, more than those by UiO-66 and ZIF-8. After composition, the distribution coefficient (K_d) and rate constant (k_2) show a 13 and 2 times increment to UiO-66, and 4469 and 10 times increment to ZIF-8. These results clearly highlight the great potential of this optimizing strategy on MOF-based composite materials for radionuclide sequestration.

To further elucidate the effect of *in situ* polymerization on the sorption efficiency, ReO_4^- sorption experiments were performed by PC_2(Cl)@MIL-101, PC_2(Cl)/*bis*-PC_2(Cl)@MIL-101, and *bis*-PC_2(Cl)@MIL-101 at diverse concentrations within 50−3000 ppm (Table S4). As the removal percentage by PC_2(Cl)@MIL-101 is normalized to 1.0 in each case (Figure 4b), with the increase of concentration for ReO_4^-, *bis*-PC_2(Cl)@MIL-101 shows a significant superiority in removal percentage. In a ReO_4^- solution at 3000 ppm, the removal percentage of *bis*-PC_2(Cl)@MIL-101 is 8 times more than that of PC_2(Cl)@MIL-101. Herein, the difference between the removal percentages of the three materials is obvious, which is due to the fact that *bis*-PC_2(Cl)@MIL-101 has a larger portion of anionic components and, thus, is more stable in solution with high ionic strength. Therefore, it is convincing that the rational fabrication of polyILs@MOFs composites can greatly

https://dx.doi.org/10.1021/acscentsci.0c01342
ACS Cent. Sci. 2020, 6, 2354−2361

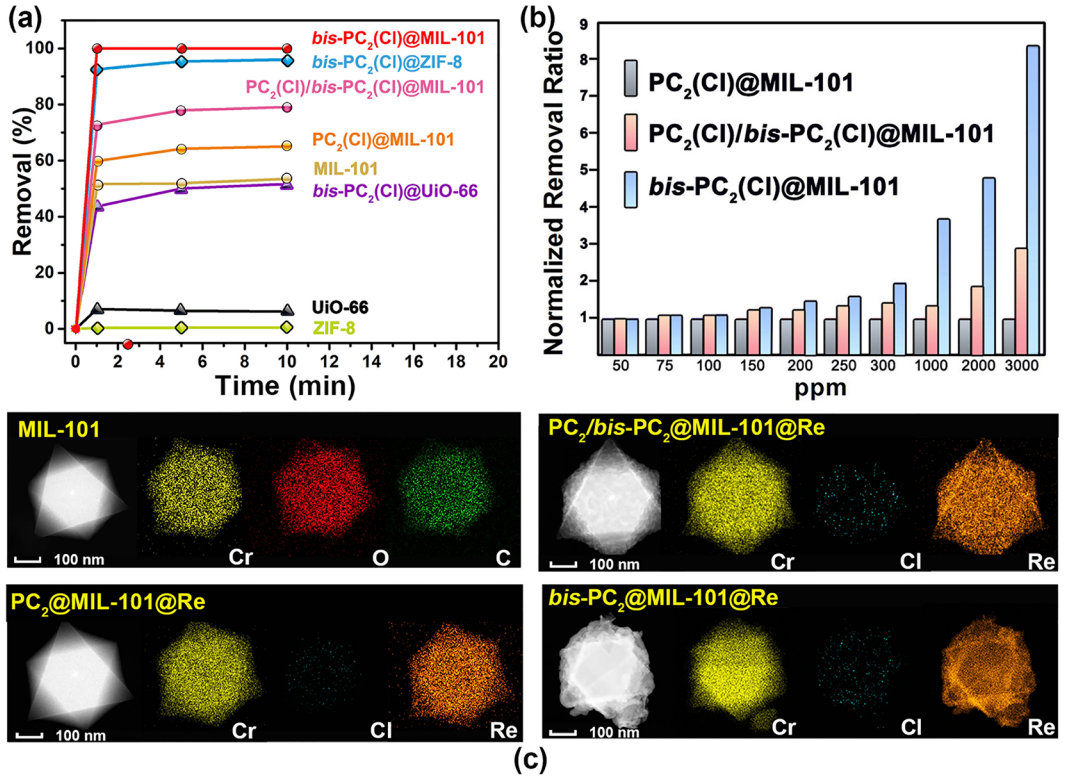

Figure 4. (a) Sorption kinetics of ReO_4^- by polyILs@MOFs and the corresponding MOFs. (b) Comparison of the sorption capacities of the ReO_4^- anion by PC_2(Cl)@MIL-101, PC_2(Cl)/*bis*-PC_2(Cl)@MIL-101, and *bis*-PC_2(Cl)@MIL-101 in ReO_4^- water solutions (50−3000 ppm). (c) STEM and EDS mapping images of MIL-101, PC_2@MIL-101@Re, PC_2/*bis*-PC_2@MIL-101@Re, and *bis*-PC_2@MIL-101@Re.

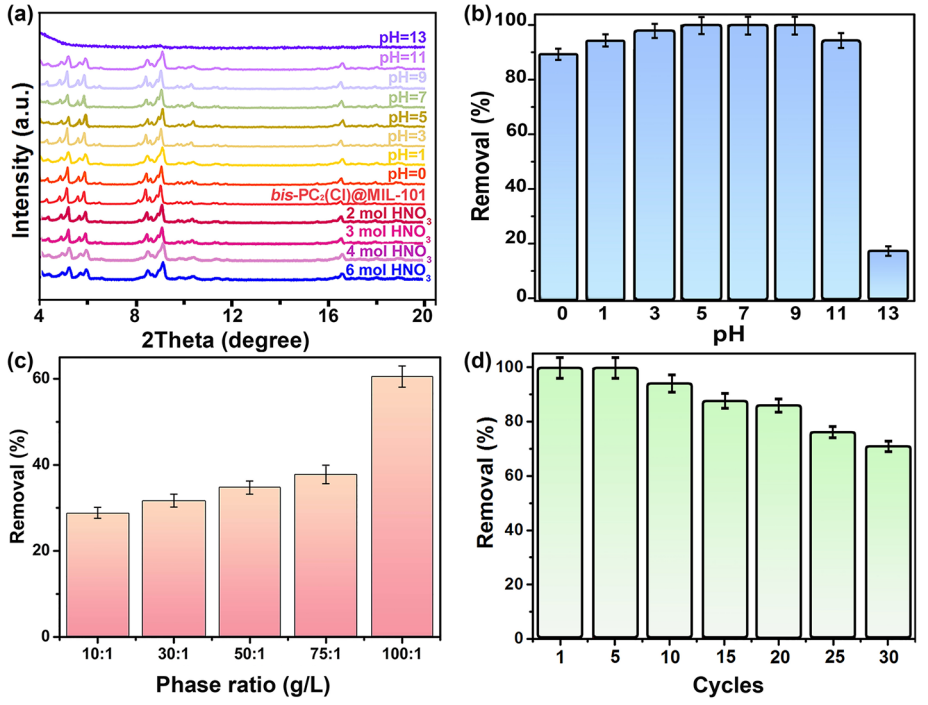

Figure 5. (a) PXRD patterns of *bis*-PC_2(Cl)@MIL-101 after immersing in the water solutions with pH values varied from 0 to 13, and in the 2, 3, 4, and 6 M HNO_3 solutions. (b) Effect of pH on the ReO_4^- sorption performances of *bis*-PC_2(Cl)@MIL-101. (c) Sorption of ReO_4^- by *bis*-PC_2(Cl)@MIL-101 as a function of solid/liquid ratio in 3 M HNO_3. (d) Recyclability of *bis*-PC_2(Cl)@MIL-101 in different sorption cycles of ReO_4^-.

enhance their working capacities toward TcO_4^-/ReO_4^- sequestration, in which both the small monomers and cross-linking polymerization are beneficial for sorption improvement.

Considering the greatly enhanced performances after polymerization, it is presumed that the high density of anion-exchange sites and the coating of cross-linked polyILs

https://dx.doi.org/10.1021/acscentsci.0c01342
ACS Cent. Sci. 2020, 6, 2354−2361

on MOFs are the fundamental contributors to the high ReO_4^- sorption efficiency of polyILs@MOFs. As shown in the STEM-EDS images of MIL-101 and polyILs@MIL-101@Re (Figure 4c), the distribution of Re is significantly different along with the change of IL monomers. In the mapping image of PC_2@MIL-101@Re, the coating polymer is not found outside MIL-101, and all the Re species are inside the MIL-101 particles. For PC_2/*bis*-PC_2@MIL-101@Re, with adding the cross-linked monomers, the MIL-101 particles are partly coated by polyILs, in which the Re species are dotted. Utilization of cross-linked ILs monomers affords *bis*-PC_2@MIL-101@Re, where cross-linked polyILs, both inside and outside MIL-101 particles, could capture large amounts of ReO_4^-. In this case, it could be hypothesized that *in situ* cross-linked polymerization of suitable IL monomers across the voids of MOFs will lead to the interknitting of polyILs through the MOF networks. Moreover, the cross-linked polyILs in the composite will be sufficiently intertangled with MOFs to serve as the tough external shield, thus greatly improving the stability. Notably, it is of great importance that polyILs with cross-linked IL monomers can serve as both the filler and coating of MOF particles, which not only provide the high density of active sites but also boost the stability of polyILs@MOFs. Therefore, such composites can be generally extended to wide-ranging applications, especially under extreme conditions. Considering the superior ReO_4^- sorption capacity of *bis*-PC_2(Cl)@MIL-101, it is reasonably chosen for further investigation.

Stability and Recyclability. The stability and reusability of sorbents in extreme conditions represent the substantial prerequisite to their actual application in nuclear fuel reprocessing and waste management. As depicted in Figure 5a, the framework structure of *bis*-PC_2(Cl)@MIL-101 remains unchanged after being soaked in highly acidic (6 M HNO_3) or alkaline (pH = 11) water solution for 1 week. Accordingly, their removal percentages for ReO_4^- are >90% under pH = 0−11 (Figure 5b). In the highly alkaline solution, MIL-101 is not stable, and the digestion of composite occurs.[45] At pH = 13, *bis*-PC_2(Cl)@MIL-101 shows almost no PXRD peak, and its sorption performance is poor (ca. 20% of ReO_4^- removal) due to framework collapse. The result also reveals that the survived polyILs still show some anion-exchange ability. Although *bis*-PC_2 is known as water-soluble, the cross-linked polymerization of *bis*-PC_2 in the pores of MIL-101 can largely affect its polymerization degree and thus the solubility in water. In order to verify this hypothesis, the digestion of *bis*-PC_2@MIL-101@Re was taken, and the resultant porous floccus *bis*-PC_2@Re solids were insoluble in the solution. As shown in Figure S12, almost no Cr, Br, and Cl element can be observed in the EDS mapping, where C, N, O, and Re elements are evenly distributed. More impressively, *bis*-PC_2(Cl)@MIL-101 can maintain ca. 62% of ReO_4^- removal from 3 M HNO_3 (NO_3^-/ReO_4^- molar ratio = 1619) at a solid/liquid phase ratio of 100 g L^{-1} (Figure 5c). This ultrahigh selectivity for ReO_4^- over NO_3^- anions can be ascribed to the hydrophobic pores in *bis*-PC_2(Cl)@MIL-101 with a strong affinity to the anion of lower charge density, which is similar to MOF and polymer systems.[57−60]

Encouraged by the above results, the recyclability of *bis*-PC_2(Cl)@MIL-101 was further evaluated, which will afford great advantage as the cost-effective sorbents (the current cost of *bis*-PC_2(Cl)@MIL-101 is ∼$300 per kilogram). Notably, almost 100% ReO_4^- could be removed after five cycles, and even after 30 cycles, above 70% removal percentage is still retained (Figure 5d and Figure S13). These features show that this material is highly recyclable and thus has a great priority toward radionuclide sequestration in the real fuel repossessing conditions.

ReO_4^- Removal from Simulated Nuclear Waste. The superior sorption performance of *bis*-PC_2(Cl)@MIL-101 inspires us to study its practicability in a simulated nuclear waste solution. In the simulated Hanford LAW melter recycle stream, the amounts of NO_3^-, Cl^-, and NO_2^- ions are over 300 times more than that of the ReO_4^- ion (Table S5), which thus poses a great challenge for TcO_4^- sequestration. By adding *bis*-PC_2(Cl)@MIL-101 (20 mg) into the simulated solution (5 mL), 74% of ReO_4^- ions therein can be removed at a solid/liquid phase ratio of 4 g L^{-1}, which further reveals its great potential in practical applications.

CONCLUSION

This work establishes an optimizing strategy to greatly enhance the stability and pertechnetate sequestration for MOF-based sorbents. By *in situ* polymerization of encapsulated ILs in the pores of MOFs, the polyILs@MOF composites exhibit superior TcO_4^- removal performances compared with their MOF parents. Notably, both the smaller monomer and cross-linked polymerization are beneficial to achieve an optimal sorbent with exceptional stability under highly acidic conditions, by virtue of cross-linked polyILs as both the filler and coating of the MOF particles, the universality of which has also been testified by different MOFs. Considering the excellent stability, recyclability, sorption capacity, uptake kinetics, and the high performances in the simulated Hanford LAW melter recycle stream, the optimal *bis*-PC_2(Cl)@MIL-101 can act as a promising scavenger for $^{99}TcO_4^-$ decontamination. The result will expand the applicability of MOF-based materials for radionuclide sequestration and, further, provide a universal approach to design multifunctional composites with high activity and stability for diverse applications such as catalysis, sorption, and ion conduction.

ASSOCIATED CONTENT

Supporting Information

The Supporting Information is available free of charge at https://pubs.acs.org/doi/10.1021/acscentsci.0c01342.

Additional experimental details; figures including FT-IR spectra, PXRD patterns, pore size distribution, XPS spectra, STEM and EDS mapping images, TGA curves, sorption kinetic curves, column-chromatographic sorption images, NMR spectra; and tables including sorption results and composition of the simulated Hanford LAW melter recycle stream (PDF)

AUTHOR INFORMATION

Corresponding Author

Miao Du − *College of Chemistry, Tianjin Key Laboratory of Structure and Performance for Functional Molecules, Tianjin Normal University, Tianjin 300387, China; College of Material and Chemical Engineering, Zhengzhou University of Light Industry, Zhengzhou 450001, China;* orcid.org/0000-0002-1029-1820; Email: hxxydm@tjnu.edu.cn, dumiao@zzuli.edu.cn

https://dx.doi.org/10.1021/acscentsci.0c01342
ACS Cent. Sci. 2020, 6, 2354−2361

Authors

Cheng-Peng Li − *College of Chemistry, Tianjin Key Laboratory of Structure and Performance for Functional Molecules, Tianjin Normal University, Tianjin 300387, China;* orcid.org/0000-0002-6798-9541

Hai-Ruo Li − *College of Chemistry, Tianjin Key Laboratory of Structure and Performance for Functional Molecules, Tianjin Normal University, Tianjin 300387, China*

Jin-Yun Ai − *College of Chemistry, Tianjin Key Laboratory of Structure and Performance for Functional Molecules, Tianjin Normal University, Tianjin 300387, China*

Jing Chen − *College of Chemistry, Tianjin Key Laboratory of Structure and Performance for Functional Molecules, Tianjin Normal University, Tianjin 300387, China*

Complete contact information is available at: https://pubs.acs.org/10.1021/acscentsci.0c01342

Notes

The authors declare no competing financial interest.

■ ACKNOWLEDGMENTS

This work was financially supported by the National Natural Science Foundation of China (21771139), Tianjin Natural Science Foundation (17JCYBJC22800), and the Key Research Project of University of Henan Province (19zx004).

■ REFERENCES

(1) Attix, F. H. *Introduction to Radiological Physics and Radiation Dosimetry*; Wiley-VCH: Weinheim, Germany, 1986.

(2) Dresselhaus, M. S.; Thomas, I. L. Alternative Energy Technologies. *Nature* **2001**, *414*, 332−337.

(3) Abney, C. W.; Mayes, R. T.; Saito, T.; Dai, S. Materials for the Recovery of Uranium from Seawater. *Chem. Rev.* **2017**, *117*, 13935−14013.

(4) Ion, S. Reaction: Recycling and Generation IV Systems. *Chem.* **2016**, *1*, 663−665.

(5) Schulz, W. W.; Lombardo, N. J. *Science and Technology for Disposal of Radioactive Tank Wastes*; Plenum Press: New York, 1998.

(6) Ojovan, M. I.; Lee, W. E. *An Introduction to Nuclear Waste Immobilization*; Elsevier: Amsterdam, 2005.

(7) Lee, M.-S.; Um, W.; Wang, G. H.; Kruger, A. A.; Lukens, W. W.; Rousseau, R.; Glezakou, V.-A. Impeding ^{99}Tc(IV) Mobility in Novel Waste Forms. *Nat. Commun.* **2016**, *7*, 12067.

(8) Taylor, R. Reaction: A Role for Actinide Chemists. *Chem* **2016**, *1*, 662−665.

(9) Popova, N. N.; Tananaev, I. G.; Rovnyi, S. I.; Myasoedov, B. F. Technetium: Behaviour During Reprocessing of Spent Nuclear Fuel and in Environmental Objects. *Russ. Chem. Rev.* **2003**, *72*, 101−121.

(10) Banerjee, D.; Kim, D.; Schweiger, M. J.; Kruger, A. A.; Thallapally, P. K. Removal of TcO_4^- Ions from Solution: Materials and Future Outlook. *Chem. Soc. Rev.* **2016**, *45*, 2724−2739.

(11) Katayev, E. A.; Kolesnikov, G. V.; Sessler, J. L. Molecular Recognition of Pertechnetate and Perrhenate. *Chem. Soc. Rev.* **2009**, *38*, 1572−1586.

(12) zur Loye, H. C.; Besmann, T.; Amoroso, J.; Brinkman, K.; Grandjean, A.; Henager, C. H.; Hu, S. Y.; Misture, S. T.; Phillpot, S. R.; Shustova, N. B.; Wang, H.; Koch, R. J.; Morrison, G.; Dolgopollova, E. Hierarchical Materials as Tailored Nuclear Waste Forms: A Perspective. *Chem. Mater.* **2018**, *30*, 4475−4488.

(13) Burgeson, I. E.; Deschane, J. R.; Blanchard, D. L. Removal of Technetium from Hanford Tank Waste Supernates. *Sep. Sci. Technol.* **2005**, *40*, 201−223.

(14) *EPA Facts about Technetium-99*; U.S. EPA, 2002.

(15) King, W. D.; Hassan, N. M.; McCabe, D. J.; Hamm, L. L.; Johnson, M. E. Technetium Removal from Hanford and Savannah River Site Actual Tank Waste Supernates with Superlig® 639 Resin. *Sep. Sci. Technol.* **2003**, *38*, 3093−3114.

(16) Xiao, C.; Khayambashi, A.; Wang, S. Separation and Remediation of $^{99}TcO_4^-$ from Aqueous Solutions. *Chem. Mater.* **2019**, *31*, 3863−3877.

(17) Li, D.; Seaman, J. C.; Kaplan, D. I.; Heald, S. M.; Sun, C. J. Pertechnetate (TcO_4^-) Sequestration from Groundwater by Cost-Effective Organoclays and Granular Activated Carbon under Oxic Environmental Conditions. *Chem. Eng. J.* **2019**, *360*, 1−9.

(18) Li, D. E.; Seaman, J. C.; Murph, S. E. H.; Kaplan, D. I.; Taylor-Pashow, K.; Feng, R. F.; Chang, H.; Tandukar, M. Porous Iron Material for TcO_4^- and ReO_4^- Sequestration from Groundwater under Ambient Oxic Conditions. *J. Hazard. Mater.* **2019**, *374*, 177−185.

(19) Luo, W. S.; Kelly, S. D.; Kemner, K. M.; Watson, D.; Zhou, J. Z.; Jardine, P. M.; Gu, B. H. Sequestering Uranium and Technetium through Co-Precipitation with Aluminum in a Contaminated Acidic Environment. *Environ. Sci. Technol.* **2009**, *43*, 7516−7522.

(20) He, L.; Liu, S.; Chen, L.; Dai, X.; Li, J.; Zhang, M.; Ma, F.; Zhang, C.; Yang, Z.; Zhou, R.; Chai, Z.; Wang, S. Mechanism Unravelling for Ultrafast and Selective $^{99}TcO_4^-$ Uptake by a Radiation-Resistant Cationic Covalent Organic Framework: A Combined Radiological Experiment and Molecular Dynamics Simulation Study. *Chem. Sci.* **2019**, *10*, 4293−4305.

(21) Sun, Q.; Aguila, B.; Ma, S. Opportunities of Porous Organic Polymers for Radionuclide Sequestration. *Trends Chem.* **2019**, *1*, 292−303.

(22) Oliver, S. R. J. Cationic Inorganic Materials for Anionic Pollutant Trapping and Catalysis. *Chem. Soc. Rev.* **2009**, *38*, 1868−1881.

(23) Ravi, A.; Oshchepkov, A. S.; German, K. E.; Kirakosyan, G. A.; Safonov, A. V.; Khrustalev, V. N.; Kataev, E. A. Finding a Receptor Design for Selective Recognition of Perrhenate and Pertechnetate: Hydrogen vs. Halogen Bonding. *Chem. Commun.* **2018**, *54*, 4826−4829.

(24) Alberto, R.; Bergamaschi, G.; Braband, H.; Fox, T.; Amendola, V. $^{99}TcO_4^-$: Selective Recognition and Trapping in Aqueous Solution. *Angew. Chem., Int. Ed.* **2012**, *51*, 9772−9776.

(25) Wang, S.; Alekseev, E. V.; Juan, D. W.; Casey, W. H.; Phillips, B. L.; Depmeier, W.; Albrecht-Schmitt, T. E. NDTB-1: A Supertetrahedral Cationic Framework That Removes TcO_4^- from Solution. *Angew. Chem., Int. Ed.* **2010**, *49*, 1057−1060.

(26) Wang, S.; Yu, P.; Purse, B. A.; Orta, M. J.; Diwu, J.; Casey, W. H.; Phillips, B. L.; Alekseev, E. V.; Depmeier, W.; Hobbs, D. T.; Albrecht-Schmitt, T. E. Selectivity, Kinetics, and Efficiency of Reversible Anion Exchange with TcO_4^- in a Supertetrahedral Cationic Framework. *Adv. Funct. Mater.* **2012**, *22*, 2241−2250.

(27) Amendola, V.; Bergamaschi, G.; Boiocchi, M.; Alberto, R.; Braband, H. Fluorescent Sensing of ^{99}Tc Pertechnetate in Water. *Chem. Sci.* **2014**, *5*, 1820−1826.

(28) Long, K. M.; Goff, G. S.; Ware, S. D.; Jarvinen, G. D.; Runde, W. H. Anion Exchange Resins for the Selective Separation of Technetium from Uranium in Carbonate Solutions. *Ind. Eng. Chem. Res.* **2012**, *51*, 10445−10450.

(29) Wilmarth, W. R.; Lumetta, G. J.; Johnson, M. E.; Poirier, M. R.; Thompson, M. C.; Suggs, P. C.; Machara, N. P. Review: Waste-Pretreatment Technologies for Remediation of Legacy Defense Nuclear Wastes. *Solvent Extr. Ion Exch.* **2011**, *29*, 1−48.

(30) Fei, H.; Bresler, M. R.; Oliver, S. R. J. A New Paradigm for Anion Trapping in High Capacity and Selectivity: Crystal-to-Crystal Transformation of Cationic Materials. *J. Am. Chem. Soc.* **2011**, *133*, 11110−11113.

(31) Gándara, F.; Perles, J.; Snejko, N.; Iglesias, M.; Gómez-Lor, B.; Gutiérrez-Puebla, E.; Monge, M. Á. Layered Rare-Earth Hydroxides: A Class of Pillared Crystalline Compounds for Intercalation Chemistry. *Angew. Chem., Int. Ed.* **2006**, *45*, 7998−8001.

(32) Desai, A. V.; Manna, B.; Karmakar, A.; Sahu, A.; Ghosh, S. K. A Water-Stable Cationic Metal−Organic Framework as a Dual

Adsorbent of Oxoanion Pollutants. *Angew. Chem., Int. Ed.* **2016**, *55*, 7811−7815.
(33) Zhu, L.; Sheng, D.; Xu, C.; Dai, X.; Silver, M. A.; Li, J.; Li, P.; Wang, Y.; Wang, Y.; Chen, L.; Xiao, C.; Chen, J.; Zhou, R.; Zhang, C.; Farha, O. K.; Chai, Z.; Albrecht-Schmitt, T. E.; Wang, S. Identifying the Recognition Site for Selective Trapping of $^{99}TcO_4^-$ in a Hydrolytically Stable and Radiation Resistant Cationic Metal−Organic Framework. *J. Am. Chem. Soc.* **2017**, *139*, 14873−14876.
(34) Sheng, D.; Zhu, L.; Dai, X.; Xu, C.; Li, P.; Pearce, C. I.; Xiao, C.; Chen, J.; Zhou, R.; Duan, T.; Farha, O. K.; Chai, Z.; Wang, S. Successful Decontamination of $^{99}TcO_4^-$ in Groundwater at Legacy Nuclear Sites by a Cationic Metal−Organic Framework with Hydrophobic Pockets. *Angew. Chem., Int. Ed.* **2019**, *58*, 4968−4972.
(35) Mei, L.; Li, F.; Lan, J.; Wang, C.; Xu, C.; Deng, H.; Wu, Q.; Hu, K.; Wang, L.; Chai, Z.; Chen, J.; Gibson, J. K.; Shi, W. Anion-Adaptive Crystalline Cationic Material for $^{99}TcO_4^-$ Trapping. *Nat. Commun.* **2019**, *10*, 1532.
(36) Li, J.; Wang, X.; Zhao, G.; Chen, C.; Chai, Z.; Alsaedi, A.; Hayat, T.; Wang, X. Metal−Organic Framework-based Materials: Superior Adsorbents for the Capture of Toxic and Radioactive Metal Ions. *Chem. Soc. Rev.* **2018**, *47*, 2322−2356.
(37) Li, C. P.; Zhou, H.; Chen, J.; Wang, J. J.; Du, M.; Zhou, W. A Highly Efficient Coordination Polymer for Selective Trapping and Sensing of Perrhenate/Pertechnetate. *ACS Appl. Mater. Interfaces* **2020**, *12*, 15246−15254.
(38) Li, C. P.; Zhou, H.; Wang, J. J.; Liu, B. L.; Wang, S.; Yang, X.; Wang, Z. L.; Liu, C. S.; Du, M.; Zhou, W. Z. Mechanism-Property Correlation in Coordination Polymer Crystals toward Design of a Superior Sorbent. *ACS Appl. Mater. Interfaces* **2019**, *11*, 42375−42384.
(39) Gao, L.; Li, C.-Y. V.; Chan, K.-Y.; Chen, Z.-N. Metal−Organic Framework Threaded with Aminated Polymer Formed in Situ for Fast and Reversible Ion Exchange. *J. Am. Chem. Soc.* **2014**, *136*, 7209−7212.
(40) Gao, L.; Li, C.-Y. V.; Chan, K.-Y. Polystyrenesulfonate Threaded in MIL-101Cr(III): A Cationic Polyelectrolyte Synthesized Directly into a Metal−Organic Framework. *Chem. Mater.* **2015**, *27*, 3601−3608.
(41) Banerjee, D.; Elsaidi, S. K.; Aguila, B.; Li, B.; Kim, D.; Schweiger, M. J.; Kruger, A. A.; Doonan, C. J.; Ma, S.; Thallapally, P. K. Removal of Pertechnetate-Related Oxyanions from Solution Using Functionalized Hierarchical Porous Frameworks. *Chem. - Eur. J.* **2016**, *22*, 17581−17584.
(42) Liang, J.; Chen, R. P.; Wang, X. Y.; Liu, T. T.; Wang, X. S.; Huang, Y. B.; Cao, R. Postsynthetic Ionization of An Imidazole-Containing Metal−Organic Framework for the Cycloaddition of Carbon Dioxide and Epoxides. *Chem. Sci.* **2017**, *8*, 1570−1575.
(43) Khan, N. A.; Hasan, Z.; Jhung, S. H. Ionic liquid@MIL-101 Prepared via the Ship-in-Bottle Technique: Remarkable Adsorbents for the Removal of Benzothiophene from Liquid Fuel. *Chem. Commun.* **2016**, *52*, 2561−2564.
(44) Tharun, J.; Bhin, K.-M.; Roshan, R.; Kim, D. W.; Kathalikkattil, A. C.; Babu, R.; Ahn, H. Y.; Won, Y. S.; Park, D.-W. Ionic Liquid Tethered Post Functionalized ZIF-90 Framework for the Cyclo-addition of Propylene Oxide and CO_2. *Green Chem.* **2016**, *18*, 2479−2487.
(45) Ding, M.; Jiang, H.-L. Incorporation of Imidazolium-Based Poly(ionic liquid)s into a Metal−Organic Framework for CO_2 Capture and Conversion. *ACS Catal.* **2018**, *8*, 3194−3201.
(46) Aguila, B.; Sun, Q.; Wang, X.; O'Rourke, E.; Al-Enizi, A. M.; Nafady, A.; Ma, S. Lower Activation Energy for Catalytic Reactions through Host-Guest Cooperation within Metal−Organic Frameworks. *Angew. Chem., Int. Ed.* **2018**, *57*, 10107−10111.
(47) Kinik, F. P.; Uzun, A.; Keskin, S. Ionic Liquid/Metal−Organic Framework Composites: From Synthesis to Applications. *ChemSusChem* **2017**, *10*, 2842−2863.
(48) Sun, Y.; Huang, H.; Vardhan, H.; Aguila, B.; Zhong, C.; Perman, J. A.; Al-Enizi, A. M.; Nafady, A.; Ma, S. Facile Approach to Graft Ionic Liquid into MOF for Improving the Efficiency of CO_2 Chemical Fixation. *ACS Appl. Mater. Interfaces* **2018**, *10*, 27124−27130.
(49) Rogers, R. D.; Seddon, K. R. Ionic Liquids-Solvents of the Future? *Science* **2003**, *302*, 792−793.
(50) Zhang, S.; Zhang, J.; Zhang, Y.; Deng, Y. Nanoconfined Ionic Liquids. *Chem. Rev.* **2017**, *117*, 6755−6833.
(51) Khan, N. A.; Hasan, Z.; Jhung, S. H. Ionic Liquids Supported on Metal−Organic Frameworks: Remarkable Adsorbents for Adsorptive Desulfurization. *Chem. - Eur. J.* **2014**, *20*, 376−380.
(52) Fujie, K.; Kitagawa, H. Ionic Liquid Transported into Metal−Organic Frameworks. *Coord. Chem. Rev.* **2016**, *307*, 382−390.
(53) Yoshida, Y.; Kitagawa, H. Ionic Conduction in Metal−Organic Frameworks with Incorporated Ionic Liquids. *ACS Sustainable Chem. Eng.* **2019**, *7*, 70−81.
(54) Li, Z.; Wang, W.; Chen, Y.; Xiong, C.; He, G.; Cao, Y.; Wu, H.; Guiver, M. D.; Jiang, Z. Constructing Efficient Ion Nanochannels in Alkaline Anion Exchange Membranes by the in situ Assembly of a Poly(ionic liquid) in Metal−Organic Frameworks. *J. Mater. Chem. A* **2016**, *4*, 2340−2348.
(55) Sun, Y.; Jia, X.; Huang, H.; Guo, X.; Qiao, Z.; Zhong, C. Solvent-Free Mechanochemical Route for the Construction of Ionic Liquid and Mixed-Metal MOF Composites for Synergistic CO_2 Fixation. *J. Mater. Chem. A* **2020**, *8*, 3180−3185.
(56) Liu, Z. W.; Han, B. H. Evaluation of an Imidazolium-Based Porous Organic Polymer as Radioactive Waste Scavenger. *Environ. Sci. Technol.* **2020**, *54*, 216−224.
(57) Li, J.; Dai, X.; Zhu, L.; Xu, C.; Zhang, D.; Silver, M. A.; Li, P.; Chen, L.; Li, Y.; Zuo, D.; Zhang, H.; Xiao, C.; Chen, J.; Diwu, J.; Farha, O. K.; Albrecht-Schmitt, T. E.; Chai, Z.; Wang, S. $^{99}TcO_4^-$ Remediation by a Cationic Polymeric Network. *Nat. Commun.* **2018**, *9*, 3007.
(58) Sun, Q.; Zhu, L.; Aguila, B.; Thallapally, P. K.; Xu, C.; Chen, J.; Wang, S.; Rogers, D.; Ma, S. Optimizing Radionuclide Sequestration in Anion Nanotraps with Record Pertechnetate Sorption. *Nat. Commun.* **2019**, *10*, 1646.
(59) Zhu, L.; Xiao, C.; Dai, X.; Li, J.; Gui, D.; Sheng, D.; Chen, L.; Zhou, R.; Chai, Z.; Albrecht-Schmitt, T. E.; Wang, S. Exceptional Perrhenate/Pertechnetate Uptake and Subsequent Immobilization by a Low-Dimensional Cationic Coordination Polymer: Overcoming the Hofmeister Bias Selectivity. *Environ. Sci. Technol. Lett.* **2017**, *4*, 316−322.
(60) Banerjee, D.; Xu, W. Q.; Nie, Z. M.; Johnson, L. E. V.; Coghlan, C.; Sushko, M. L.; Kim, D.; Schweiger, M. J.; Kruger, A. A.; Doonan, C. J.; Thallapally, P. K. Zirconium-Based Metal−Organic Framework for Removal of Perrhenate from Water. *Inorg. Chem.* **2016**, *55*, 8241−8243.

https://dx.doi.org/10.1021/acscentsci.0c01342
ACS Cent. Sci. 2020, 6, 2354−2361